Proceedings World Geothermal Congress 2026
Calgary, Canada, June 8 – 11, 2026

# Geochemical Assessment of the Picard River Geothermal Prospect in Northern Dominica

Kenneth B. Alexander[1]*, Scott W. Herman[2] and Andrew P.G. Fowler[3]
Middle Earth Geoscience[1]*, Vulcan Geoscience[2], EHS-Support[3]
*Keg@middleearth-geo.com

**Keywords:** geochemical assessment, submarine hot spring sampling, multicomponent thermodynamic geothermometry, Picard River, Dominica

## ABSTRACT

This paper discusses the methods and results of a geochemical survey conducted in April-May 2024 as part of a supplemental resource assessment of the Picard River prospect in northern Dominica. It is one of several programs funded by the NZ Caribbean Facility for Renewable Energy (FRENZ), which is supported by the Ministry of Foreign Affairs (MFAT). Fieldwork involved geological and geochemical surveys, including innovative techniques such as sampling of submarine hot springs and multicomponent thermodynamic geothermometry (MTG). The FRENZ technical team collected water samples from terrestrial and submarine hot springs. The submarine springs, which discharged water at temperatures between 124-128°C, were sampled at depths between 25 and 28 m. This is essentially equivalent to pressure in a >30-m deep borehole onshore that follows the boiling point with depth curve. As such, the submarine springs provide the most valid sampling points of the Picard River geothermal system reservoir outflow. The FRENZ technical team successfully removed the seawater component from the submarine water samples using geochemical modelling software. This approach yielded a high-quality MTG analysis, providing a more precise range of reservoir temperatures for the submarine springs. The new range spans approximately 220 to 240°C, significantly narrowing the previous range of 163 to 270°C, which was determined based on classical geothermometry analysis on diluted terrestrial spring water samples collected in 2009. The geochemical analytical results of the water samples, both historical and current, indicate three different water types, consistent with the hydrological model typical of a high-elevation, andesitic island-arc hydrothermal system.

## 1 INTRODUCTION

Geothermal exploration surveys conducted in 2008 (Rohrs, 2009) and 2020-22 (Jacobs, 2023) revealed evidence of a potential high-temperature resource in northern Dominica's Picard River area (Figure 1). The Picard River geothermal system is a greenfield site – no wells have been drilled.

In April-May 2024, the FRENZ technical team completed geological and geochemical surveys including analysis of remote imaging, a field geology survey, an inventory of thermal manifestations, and geochemical sampling and analysis of known onshore and offshore features.

## 2 GEOLOGY – STRUCTURAL SETTING

The geology of northern Dominica is dominated by the 1,421-m high Morne Diablotins andesitic volcano. Pyroclastic-flow deposits, emplaced ~22,000-46,000 years ago, extend in radial lobes as far as the coast (Smith et al., 2013). These ignimbrite deposits represent the most recent volcanic activity of Morne Diablotins.

During April-May 2024, the FRENZ technical team completed a geological field survey, which consisted of field observations of the very limited outcrops in the northern Dominica area of interest. It is difficult to discern structures in the field in Dominica, due to the combination of rough terrain, heavy vegetation, and dense human development in certain areas.

Much of the bedrock is obscured in most places, limiting the accessible outcrops to streambeds and road cuts, meaning that many structures must be inferred from the few outcrops and the morphology of the terrain. In Dominica, offshore structures can sometimes be correlated with mapped onshore faults. Feuillet et al (2002) documented the existence of multiple submarine volcanic centers controlled in part by the presence of several NW-striking submarine faults that extend to the NW offshore of northern Dominica (Figure 2). The southernmost of these faults extends through the study area to the peak of Morne Diablotins, and which we will refer to as the Morne Diablotins Fault Zone (MDFZ).

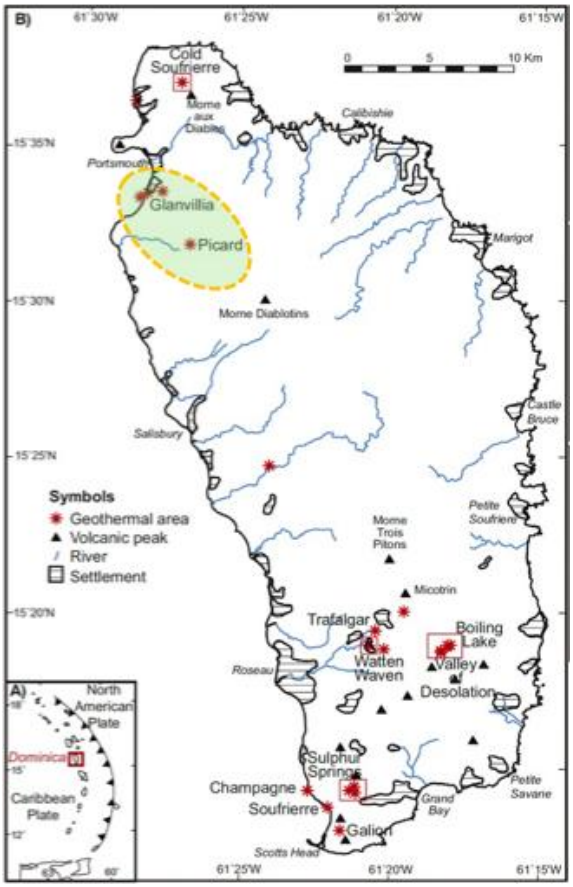



**Figure 1. A) Inset map of the Lesser Antilles showing the location of Dominica, and B) map of Dominica highlighting geothermal areas (Joseph et al., 2019).**

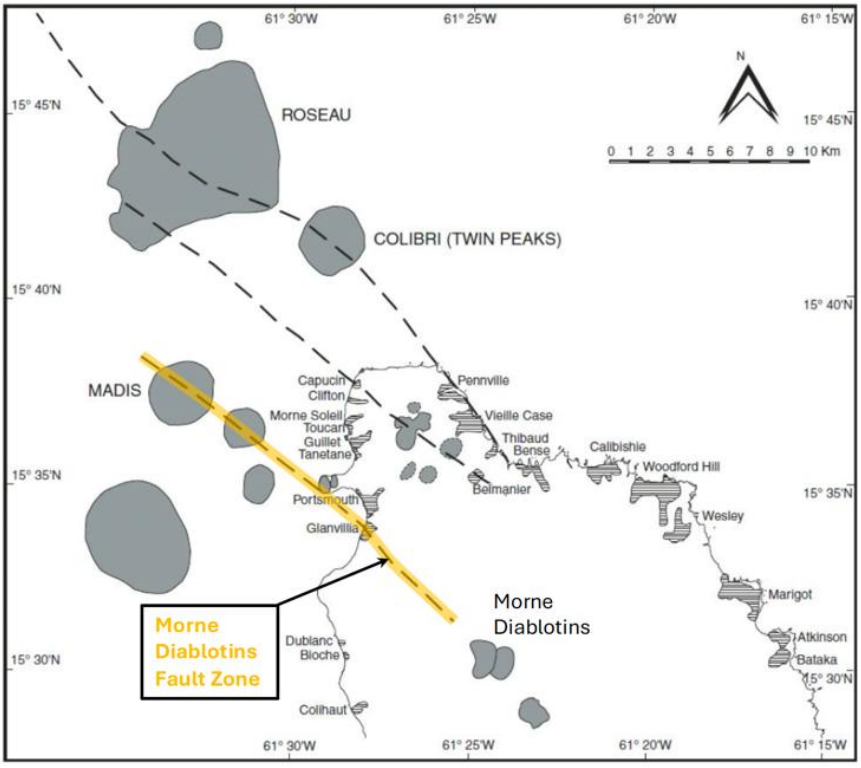



**Figure 2. Distribution of volcanic centers and submarine faults with their on-land extensions (modified from Smith et al., 2013).**

The distribution of the geothermal surface features associated with the Picard River geothermal system appears to be largely controlled by the inferred MDFZ, which runs along the northern boundary of the interpreted flank collapse (Figure 3). The Upper Picard River warm springs, the only geothermal manifestation found on the volcano's flanks, lie along the fault at or near the intersection with the head scarp of the flank-collapse feature. This logical connection is based on the expectation that the top of the flank-collapse feature, near the head, would contain extensional structures that would facilitate the upflow of geothermal fluids.

One possible explanation for the distribution of geothermal manifestations is that the Morne Diablotins strike-slip fault plays a dominant role in determining their location. The MDFZ, a seafloor strike-slip fault that coincides with the northern boundary of the flank collapse, is expected to penetrate the entire volcanic massif and into any underlying geothermal reservoir. This permeable pathway would facilitate the upflow of geothermal fluids.




**Figure 3. Distribution of geothermal features in the Picard River geothermal system. View looking east. Orange line is the inferred Morne Diablotins Fault Zone, yellow line is the boundary of the interpreted flank collapse feature, and red lines are the areas of shifting hot water seeps in the sand along the shore.**

## 3 THERMAL FEATURES – OFFSHORE AND ONSHORE

In April and May 2024, the FRENZ technical team inventoried the geothermal features associated with the Picard River geothermal system. The geothermal surface features are mainly located in the southern half of Prince Rupert Bay, extending to Pointe Ronde (Figure 3). These features include two areas of submarine springs in Prince Rupert Bay and two more areas of submarine springs along Pointe Ronde, two stretches of shoreline or beach with shifting hot water seeps in the tidal zone, and eight known onshore locations within and around the community of Picard. Thermal features are summarized in Table 1.

Most of the onshore and offshore thermal springs are aligned along the major NW-SE MDFZ, which is co-located with the northern boundary of the interpreted flank collapse (Figure 3). The strong NW-SE alignment of springs suggests that fluid flow is likely controlled by fracture permeability along active faults. Moving from NW to SE (offshore to onshore), the FRENZ technical team observed the following thermal manifestations associated with the Picard River geothermal system:

**Table 1. Summary of thermal features associated with the Picard River geothermal system.**

| | | | | | | Temperature (°C) | |
|---|---|---|---|---|---|---|---|
| Name | Feature type | Water type | Latitude | Longitude | Elev (masl) | FRENZ (2024) | Smith et al (2013) |
| Volcano submarine | Submarine hot springs | Cl brine | 15.56345° | -61.46521° | -25 | NA | 124 |
| Hot Sophia submarine | Submarine hot springs | Cl brine | 15.55273° | -61.46820° | -27 | NA | 128 |
| Prince Rupert Bay submarine | Submarine hot springs | Unknown | Locations vary, 0.2-1.9 km S of Picard R. | | Intertidal | NA | NA |
| Picard River mouth | Hot springs | Cl brine | 15.56111° | -61.45914° | 2 | Dry | 94-101 |
| Mamie's | Warm springs | Cl brine | 15.55275° | -61.45842° | 14 | 41.4 | 56 |
| Avie's Villa | Hot springs | Cl brine | 15.55365° | -61.45686° | 30 | 63.5 | NA |
| Gloshow | Warm springs | Bicarb. | 15.56194° | -61.45121° | 51 | 47.7 | 48 |
| Balvin | Hot ground; weak solfataras | Acid sulfate | 15.55759° | -61.45214° | 35 | Dry, but hot ground | 88-95 |
| Ross Castle | Warm spring | Unknown | 15.55277° | -61.45121° | 68 | NA | NA |
| Karen | Warm spring | Cl brine | 15.54948° | -61.45564° | 86 | 30 | NA |
| Upper Picard River | Warm springs | Acid sulfate | 15.52261° | -61.41471° | 579 | NA | 33-34 |

### 3.1 Volcano submarine hot spring

Approximately 550 m offshore from the mouth of the Picard River, there is an area of submarine hot springs. It lies along the path of a series of PVC pipes that were installed offshore by the river mouth as part of a local aquaculture effort that was destroyed by Hurricane Maria in 2017. There are many depressions in an area of bare sand, giving the impression that there are multiple spring vents (only some were flowing). Water samples collected from these springs were surrounded by thin yellow sulfur deposits and smelled strongly of sulfur when brought to the surface.

### 3.2 Hot Sophia submarine hot spring

Likely the same feature as the previously reported Black Coral hot spring. A large patch of bare sand with numerous small (0.5-1 m wide) shallow (~10 cm) depressions surrounded by thin yellow sulfur deposits. Hot water exits from some of the depressions, but not all, in varying amounts. It appears the water periodically changes exit points throughout the bare area, resulting in constantly shifting springs in an overall stable area of discharge. Springs were found at the same approximate location in 2006 and again in 2024.

### 3.3 Southern Prince Rupert Bay submarine hot springs

These springs or seeps are located within a few hundred m of the coastline over a stretch of beach south of the Picard River. Several residents and previous researchers reported feeling various hot spots in the sand along the southern half of Prince Rupert Bay, extending south of the Picard River to the end of the beach that backs Secret Bay Resort.

### 3.4 Picard River mouth hot springs

Two hot springs on the south shore of the Picard River, near the river mouth. Both emerge at the current water level from the sand and boulders making up the southern shore of the river. Past researchers measured these springs at 98°C with sufficient flow for sampling. However, during our visit, we found only areas of hot sand at (~75°C) with no discernible flow.

### 3.5 Mamie's warm spring

Warm water collected in concrete pool at abandoned resort destroyed by the Category 4 Hurricane Maria (2017). Pool is now full of vegetation debris with no flow or indication of the source of the spring.

### 3.6 Avie's Ville hot spring

Hot spring emerging from a fissure in the hillside that wraps around the back of Avie's Ville resort and lies at the NE corner of the pool area at the base of some trees. The outflow of the fissure has been walled in to form a small pool, which is piped to a hot tub at the other end of the swimming pool.

### 3.7 Gloshow hot spring

A warm spring issuing from a rock face on the northern side of the streambed, about 1 m above the stream level. There is a soaking pool consisting of large boulders around a sandy bottomed pool.

### 3.8 Balvin hot ground and possible solfataras

An area of hot ground and no vegetation within a forested grove east of the driveway in Kootney Resorts. It lies 110 meters north of the Picard River and 1-2 meters above the river level. In April 2024, the FRENZ technical team detected a faint sulfur smell at a few depressions where steam had previously emanated, but no discernible flow. A 2-m PVC pipe pushed into the ground by hand and removed was covered with steaming mud, confirming extensive clay alteration. The feature exhibits seasonal and yearly variations, primarily influenced by the level of moisture. During wet seasons or years, solfatara activity intensifies, resulting in hot water into the drainage ditch.

### 3.9 Ross Castle warm springs

Several locals informed us that before Hurricane Maria, there were several warm springs that emerged from the north shore of the Picard River, along the Ross Castle stretch, between the point where the road curves away from the river and up to the suspension foot bridge. However, during Hurricane Maria, the riverbed was extensively altered due to the flooding, and the old springs have disappeared. Despite several locals claiming that the springs still exist, the FRENZ technical team was unable to locate them.

### 3.10 Karen warm spring

Cement and stone pool with warm water piped in from ravine behind the pool. PVC pipe appears to be driven into the earth in the ravine, and the warm water emerges from the pipe. No indication of source of spring found.

### 3.11 Upper Picard warm springs

These springs, reportedly located along the Picard River below the Syndicate Nature Trail overlook, were previously sampled by Rohrs (2009) and Smith et al. (2013). In April/May 2024, the FRENZ technical team were unable to locate the springs despite extensive efforts and the assistance of local guides. It is possible that the springs have been covered over or destroyed by the reworking of the streambed during Hurricane Maria.

## 4 GEOCHEMISTRY - WATER SAMPLING AND GEOTHERMOMETRY

During the April/May 2024 field surveys, the FRENZ technical team collected water samples from two terrestrial hot springs (Gloshow and Avie's) and two submarine hot springs (Volcano and Hot Sophia). Submarine samples were collected at depths between 25 and 28 m, which are essentially equivalent to pressure in a >30-m deep borehole onshore that follows the boiling with depth curve. This is because 25 m of overlying cold seawater is much denser than hot water in inshore geothermal systems. Although the submarine springs are mixed with seawater, the composition of seawater is well defined, and methods to back out the mixing are well established and accepted having been utilized in virtually every study of submarine hot springs since the early 1980s. As such, the submarine springs provide the most valid sampling point of the Picard River geothermal system reservoir outflow.

Three water samples were collected from each submarine hot spring and from different vents at each area (Figure 4). A weighted funnel was set over the vent, and a peristaltic hand pump was used to transfer the fluid from the funnel into a 10-L collapsible water bag. This was then closed off and taken to the surface where a single sample was divided into the various sample bottles of a sample set on the dive boat.

The three samples collected per submarine site, plus an unaltered seawater sample, provided varying degrees of seawater mixing that allowed us to calculate a Mg regression line that was used to 'back out' the sea water component from the submarine water samples using geochemical modelling software. This process allowed us to model a theoretical unmixed (with seawater) reservoir fluid that could then be used for multicomponent thermodynamic geothermometry (MTG), thereby providing a significantly more precise temperature estimate of the original geothermal reservoir fluids.



**Figure 4. FRENZ technical team (Scott Herman) collecting water sample at Volcano submarine hot spring at a depth of 25 m.**

### 4.1 Water types

The geochemical analytical results of the water samples, both historical and current, indicate three different water types, consistent with the hydrological model typical of a high-elevation, andesitic island-arc hydrothermal system. For the Picard River geothermal system, sodium-chloride water is found at the two submarine springs, as well as terrestrial springs at the Picard River mouth, Avie's, and Mamie's (Figure 5). These springs are farthest away (>8 km) from the presumed upflow beneath Morne Diablotins and are indicative of the extensive lateral outflow, which is typical of these types of systems.

The Gloshow warm springs are the only thermal feature of the Picard River geothermal system with bicarbonate water. Gloshow is the farthest north of the Glanvillia springs and located north of the Morne Diablotins Fault Zone (Figure 7). The bicarbonate water at Gloshow is consistent with its location on the marginal part of a liquid-dominated system.

Acid-sulfate waters are found at Upper Picard River (Figure 5). The weak solfataras and extensive clay alteration at Balvin are also indicative of acid-sulfate water type, although no springs are present at Balvin. These acid-sulfate features are evidence of potential upflows on the flanks of Morne Diablotins (Upper Picard River) and near-surface outflow at Balvin in the Glanvillia springs area.

### 4.2 Analytical data calculation for submarine water samples

The Picard River geothermal system's submarine hot springs, Hot Sophia and Volcano, offer a glimpse into deeper and less accessible subsurface regions due to the high temperatures and pressures caused by the hydrostatic pressure of overlying seawater. At depths of 25 m and 28 m, the pressures reach 3.5 and 3.8 atmospheres, respectively, with equivalent boiling points of approximately 139 and 142.5°C. These pressures make the submarine samples comparable to those collected from geothermal boreholes, making them less susceptible to re-equilibration at lower temperatures and pressures compared to subaerial hot springs. Consequently, this geochemistry assessment focuses on the submarine hot springs. However, it's important to

note that the measured temperatures of 124-128°C at these depths are below the boiling point, contrary to previous reports, as they include the sum of the water column plus the atmospheric pressure.

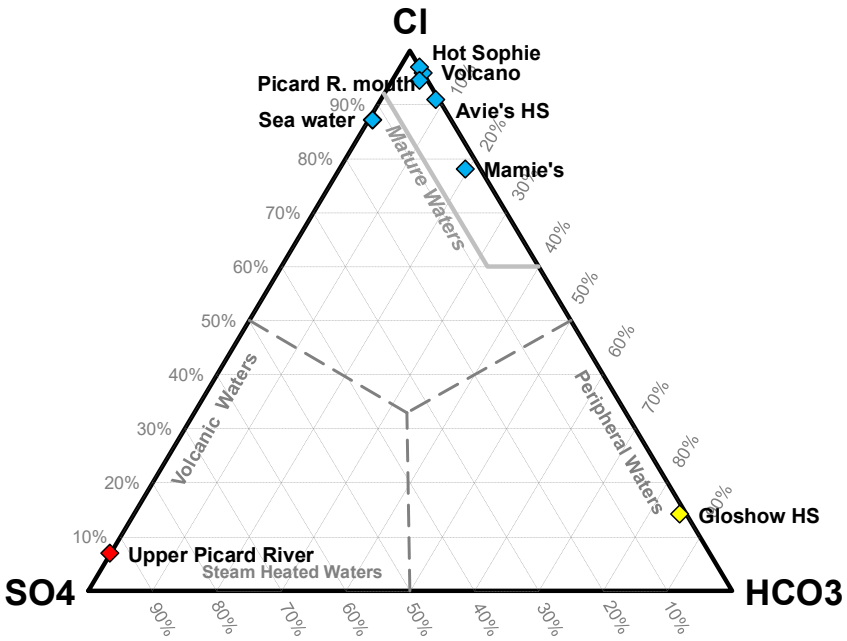



**Figure 5. A Cl-SO4-HCO3 ternary diagram showing chemical composition of the thermal features in the Picard River area (modified from Powell & Cumming, 2010). Data for Upper Picard River, Picard River mouth, and Mamie's from Rohrs (2009). Sodium-chloride waters shown by blue markers.**

At the submarine vent site, bubbles are observed exiting the vent, suggesting that non-condensable gases (NCGs) exsolved from the spring fluids at the extreme bottom pressures. Previous gas analyses in the area indicated that carbon dioxide constitutes over 90% of NCGs (Rohrs, 2009). To account for the effects of carbon dioxide degassing, Geochemists' Workbench (GWB) software (Bethke & Yeakel, 2012) was used, utilizing the standard thermodynamic database (thermo.tdat) to model carbon dioxide back into the fluids, achieving a partial pressure consistent with absolute pressure at the sampled depths.

### 4.3 Classical geothermometry results

Classical geothermometer temperatures were calculated from measured subaerial and computed endmember submarine fluid analytical results. Select analytical data from Rohrs (2009) were used to compute classical geothermometer results using the same equations as a point of comparison (Table 2). Results using high temperature geothermometer formulations for the submarine springs sampled in 2024 suggest temperatures ranging from approximately 200 to over 280°C (assuming no steam loss), consistent with results from one of the highest temperature onshore springs (Picard River mouth) sampled by Rohrs (2009).

Geothermometer results for Gloshow and Avie's onshore springs have a much wider spread, ranging from 26 to 205°C (Gloshow) and 163 to 219°C (Avie's) for the 2024 data, with similar variability in previous years. The variability in the empirical geothermometer results for onshore springs (except the lower Picard River hot springs) suggests that these results are suspect and likely affected by equilibration at lower temperatures, particularly for silica where the beta cristobalite formulation yields temperatures generally similar to the measured spring temperatures.

Classical geothermometers are an important and essential geothermal exploration tool. However, geothermal fluids ascending to ground surface are typically affected by gas loss, mixing, and/or dilution with shallower waters, masking their deep geochemical signatures. Also, equilibration with minerals of compositions different than those for which the geothermometers were formulated can lead to variable results (Spycher et al., 2014). It is noted that longer equilibration time for the Na/K geothermometer may preserve evidence of distal upflow temperatures due to longer timeframes for equilibration; however, there is evidence of boiling, degassing, and other processes occurring at the submarine springs that could affect these results. Consequently, the FRENZ team pursued a multicomponent geothermometer approach applied to the submarine spring waters that are less likely to be affected by low temperature processes due to the high temperatures.

**Table 2. Empirical geothermometer results.**

| | Rohrs (2009) | | | FRENZ (2024) | | | |
|---|---|---|---|---|---|---|---|
| Parameter | Lower PR Springs | Gloshow | Clement/ Avie's | Gloshow | Avie's Villa | Volcano | Hot Sophia |
| B | 43.30 | 0.20 | 50.5 | <0.40 | 49 | 83.36 | 79.31 |
| SiO2 | 380 | 102 | 395 | 57 | 182 | 262 | 303 |
| Li | 5.60 | 0.10 | 7.2 | <0.01 | 7.3 | 13.56 | 11.86 |
| Na | 1570 | 23 | 1960 | 23 | 2056 | 3896 | 3546 |
| K | 234 | 2 | 118 | 1.6 | 143 | 680.2 | 650.4 |
| Ca | 141 | 23 | 293 | 26 | 329 | 544 | 472 |
| Mg | 11 | 6 | 10 | 6 | 9.1 | 0.0 | 0.0 |
| Cl | 2890 | 24 | 3500 | 27 | 3671 | 7673 | 7052 |
| SO4 | 39 | 2 | 1960 | 1.8 | 20 | 0 | 0 |
| HCO3 | 133 | 120 | 326 | 162 | 350 | 246 | 308 |
| Sum Cations | 83.02 | 2.71 | 104.76 | 2.83 | 111.31 | 215.97 | 196.10 |
| Sum Anions | -84.51 | -2.69 | -144.87 | -3.45 | -109.70 | -220.447 | -203.97 |
| Charge Balance (%) | -1% | 0% | -16% | -10% | 1% | -1% | -2% |
| Measured temp (°C) | 82.2 | 43.3 | 72.2 | 47.8 | 63.6 | -- | -- |
| High T Geothermometers (°C) | | | | | | | |
| Quartz conductive | 230 | 138 | 234 | 108 | 174 | 200 | 212 |
| Quartz – steam loss | 207 | 134 | 210 | 108 | 163 | 184 | 193 |
| Na-K-Ca | 230 | 34 | 173 | 26 | 181 | 246 | 249 |
| Na/K | 254 | 205 | 177 | 188 | 188 | 270 | 275 |
| Na/K | 266 | 221 | 195 | 205 | 205 | 281 | 286 |
| Na/Li | 220 | 233 | 222 | -- | 219 | 218 | 215 |
| Low T Geothermometers (°C) | | | | | | | |
| Chalcedony Conductive | 216 | 112 | 220 | 79 | 152 | 181 | 194 |
| Alpha Cristobalite | 181 | 88 | 185 | 58 | 124 | 150 | 162 |
| Beta Cristobalite | 131 | 39 | 135 | 10 | 74 | 100 | 112 |
| Amorphous Silica | 104 | 18 | 107 | -9 | 50 | 75 | 86 |

### 4.4 Multicomponent geothermometer results

Multicomponent thermodynamic geothermometry (MTG) presents advantages over classical geothermometers because they rely on complete fluid analyses and a solid thermodynamic basis, rather than the solubility of a few minerals or (semi-) empirical correlations, and thus in principle, apply to any geochemical system (Spycher

et al., 2014). We applied an MTG-based model following the approach of Reed & Spycher (1984), using endmember fluid data obtained from the submarine Volcano and Hot Sophia hot springs. Results are shown in Figure 6 for Volcano hot springs and yield a narrow range of temperatures of 222.5 to 240°C. Hot Sophia hot springs had a similar range of 217.5 to 232.5°C. These results likely reflect the outflow reservoir temperature, and higher upflow temperatures are possible.

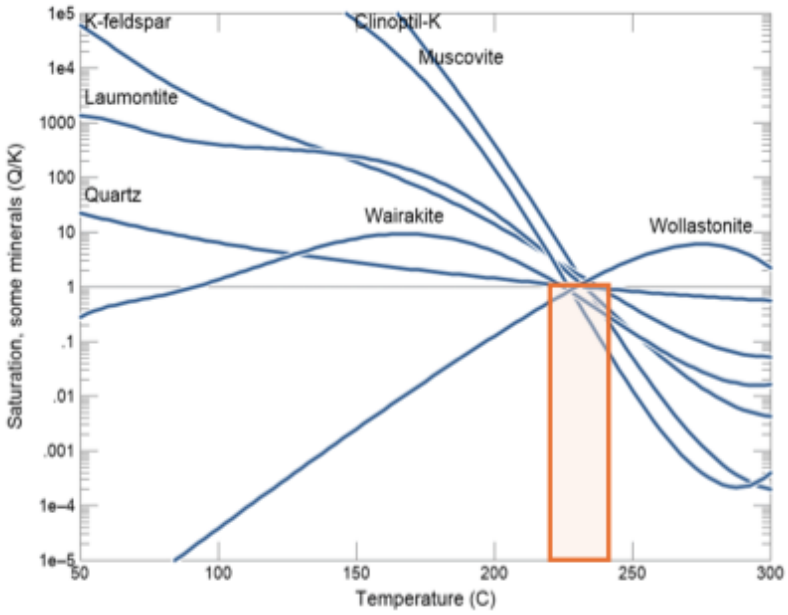



**Figure 6. Multicomponent geothermometer results for Volcano hot springs (222.5 – 240°C). The narrow range of temperatures at a saturation index of 1 is indictive of equilibrated water.**

## 5 CONCLUSIONS

During the April/May 2024 field surveys, the FRENZ technical team collected water samples from two terrestrial hot springs (Gloshow and Avie's) and two submarine hot springs (Volcano and Hot Sophia). Submarine samples were collected at depths between 25 and 28 m, which are essentially equivalent to pressure in a >30-m deep borehole onshore that follows the boiling with depth curve. As such, the submarine springs provide the most valid sampling point of the Picard River geothermal system reservoir outflow. Accordingly, the focus of this supplemental geochemistry assessment is on the submarine hot springs.

The modelling results yielded a high-quality MTG analysis with a narrow range of reservoir temperatures of 222.5 to 240°C for Volcano hot springs and 217.5 to 232.5°C for Hot Sophia hot springs (229±11°C overall). These reservoir temperature results are much more precise than the previous range of 163 to 270°C (216±54°C) based on classical geothermometry analysis on diluted terrestrial spring water samples collected from the Glanvillia area by Rohrs in 2009 (Picard River, Clement/Avie's, Mamie's). In addition, the quality of the samples and the lack of outliers among the multiple thermodynamic geothermometers gives us a high degree of confidence that we have sufficiently accounted for confounding reservoir processes that could affect the accuracy of the results.

The endmember submarine fluid compositions curiously have essentially no sulfate. Given that the onshore Balvin and Upper Picard River warm springs have pH and mineralization characteristics typical of acid-sulfate waters, it is expected that the outflow is the residue remaining following a boiling event (Figure 7). Boiling and partitioning of sulfur as non-condensable hydrogen sulfide gas into the steam phase that subsequently condenses in contact with shallow groundwater and oxidizes to sulfate creating acidity is the accepted mechanism for formation of acid-sulfate springs. A boiling event can explain the low sulfur in the boiled outflow on the seafloor; sulfur was largely quantitatively removed following a boiling event as hydrogen sulfide.

This boiling model in conjunction with the tight clustering of the multicomponent geothermometer results suggests that the outflow equilibrated along the flow path near the boiling temperature; if the result reflected pre-boiled deeper equilibration temperature, the model would have required recombining the liquid from the steam phase to achieve such consistent results. This result implies that a deeper and hotter reservoir fluid may be present hydrologically upgradient of the outflow location.

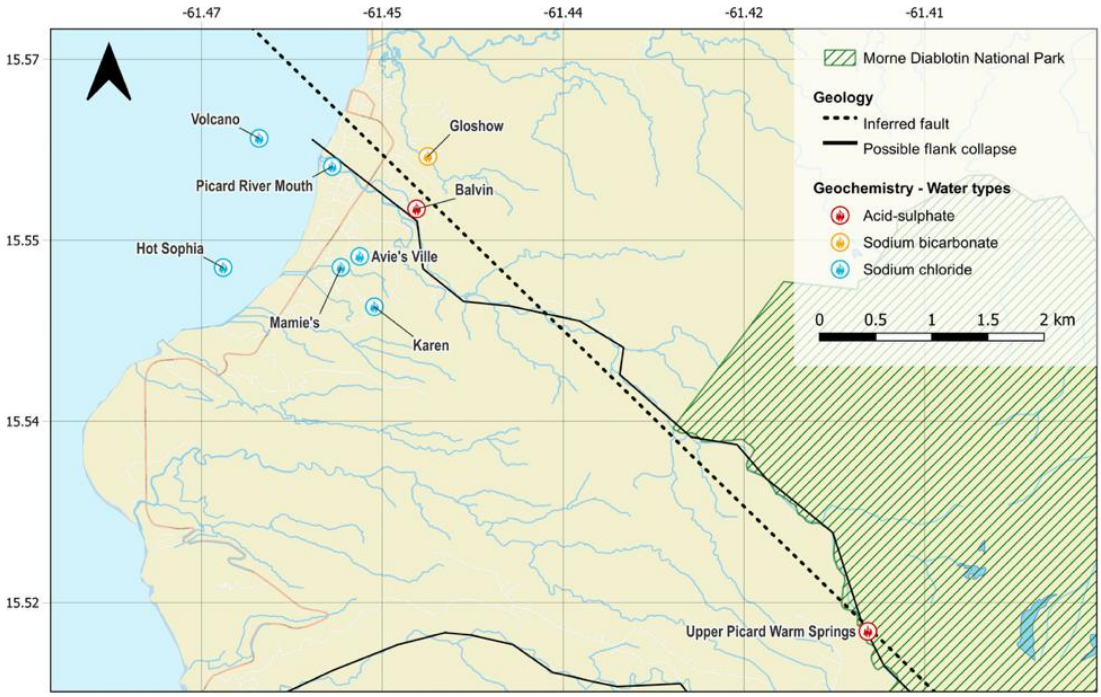



**Figure 7. Map of sampled thermal features of the Picard River geothermal system and their geochemical water types.**

**Acknowledgements**

This work is part of several programs funded by the Aotearoa New Zealand – Caribbean Facility for Renewable Energy (FRENZ), which is supported by the Ministry of Foreign Affairs (MFAT). FRENZ is delivered by Cowater International in association with JRG Energy. We also acknowledge the Green Climate Fund and the Government of the Commonwealth of Dominica for sharing their IP. We are grateful to Dave Rohrs and Prof. Alan Smith for sharing their time and detailed geoscientific knowledge of Dominica.

**REFERENCES**

Bethke, C.M. & Yeakel, S.: The Geochemist's Workbench, Release 9.0 Reaction Modeling Guide. Aqueous Solutions, LLC, (2012).

Feuillet, N., Tapponnier, P. & Manighetti, I.: Link between seismic and volcanic activity in the Lesser Antilles Arc [abs.]: Mount Pelée 1902-2002: Explosive volcanism in subduction zones, Programs and abstracts, (2002).

Jacobs New Zealand: Dominica Northern Prospect – Resource Assessment, Unpublished report No. RZ020301-FWP#6-RPT-001, prepared for Ministry of Foreign Affairs and Trade (MFAT), prepared by Jacobs New Zealand Limited, Auckland, New Zealand, (2023).

Joseph, E.P., Frey, H.M., Manon, M.R., Onyeali, M-M.C., DeFranco, K., Metzger, T. and Aragosa, C.: Update on the fluid geochemistry monitoring time series for geothermal systems in Dominica, Lesser Antilles island arc: 2009-2017, Journal of Volcanology and Geothermal Research, 376, 86-103, (2018).

Powell, T. & Cumming, W.: Spreadsheets for geothermal water and gas geochemistry, Proceedings, Thirty-fifth Workshop on Geothermal Reservoir Engineering, Stanford University, Stanford, California, February 1-3, 2010, SGP-TR-188, (2010).

Reed, M. & Spycher, N.: Calculation of pH and mineral equilibria in hydrothermal waters with application to geothermometry and studies of boiling and dilution, Geochim. Cosmochim. Acta 48, 1479-1492, (1984).

Rohrs, D.T.: Geothermal resource assessment of the Portsmouth prospect, Dominica, West Indies, unpublished report prepared by Rohrs Consulting, Inc., (2009).

Smith, A.L., Roobol, M.J., Mattioli, G.S., Fryxell, J.E., Daly, G.E. and Fernandez, L.A.: The volcanic geology of the mid-arc island of Dominica, Lesser Antilles, The Geological Society of America Special Paper, 496, (2013).

Spycher, N., Peiffer, L., Sonnenthal, E.L., Saldi, G., Reed, M.H. & Kennedy, B.M.: Integrated multicomponent solute geothermometry, Geothermics, 51, 113-123, (2014).